Supplementary Material

Carbon Framework Modification; *Interesting Strategy to Improve the Energy Storage and Dye*

Adsorption

Monika Michalska[1], Paulina Pietrzyk-Thel[2], Kamil Sobczak[3], Mathijs Janssen[4], Amrita Jain[2*]

[1]Department of Chemistry and Physico-Chemical Processes, Faculty of Materials Science and Technology, VSB-Technical University of Ostrava, 17. listopadu 2172/15, 708-00 Ostrava-Poruba, Czech Republic

[2]Institute of Fundamental Technological Research, Polish Academy of Sciences, Pawińskiego 5B, 02-106 Warsaw, Poland

[3]Faculty of Chemistry, Biological and Chemical Research Centre, University of Warsaw, Żwirki i Wigury 101, 02-089 Warsaw, Poland

[4]Norwegian University of Life Sciences, Faculty of Science and Technology, Pb 5003, 1433 Ås

[*]Corresponding author: ajain@ippt.pan.pl

Figure S1: EDX spectra of ACCu1 sample.
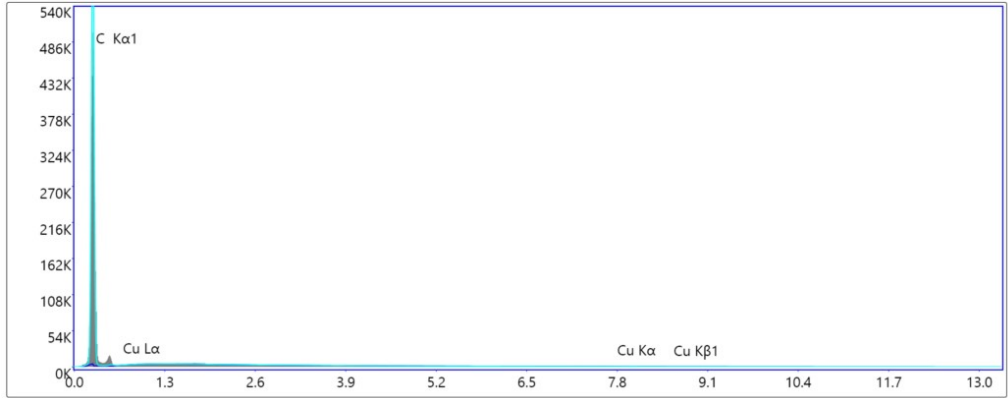
Element	Weight %	Atomic %	Error %	Kratio	Z	A	F
C K	99,8	100,0	1,1	0,9880	1,0005	0,9897	1,0000
CuK	0,2	0,0	12,3	0,0027	0,6947	1,0230	1,6584

Figure S2: N_2 adsorption spectra with pore size distribution of commercial activated carbon (AC) sample.
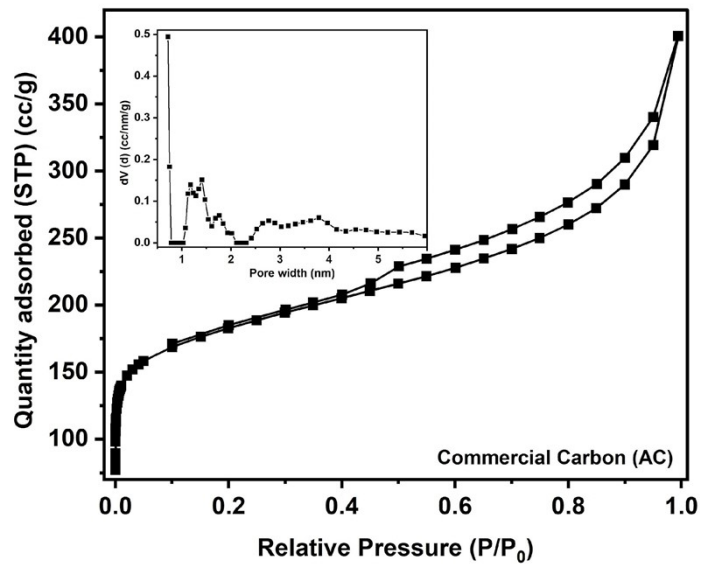
In the main text, we mentioned the lin-KK method of the impedance.py package, which we used to check the validity of our EIS data. This method fits a Voigt model to the data, cell A needed N; we set the c parameter to 0.85 (the default) elements.

In the mid-frequency range of the complex plane plots, we see that the Warburg 45 degrees behavior is too shallow. Better fits are possible in this frequency range if we replace the Warburg element, derived for planar diffusion, by its spherical diffusion counterpart (see figure 4 of [1]). However, it is unclear why spherical diffusion should be relevant for our electrodes.

Circuits very similar to ours are in Lasia's book[2], and there, the series resistance is considered a charge transfer resistance. However, the CV curves of our cells being reversible, this resistance cannot be associated with charge transfer reaction. We have also fitted our data with circuits without this resistance but with modified Bisquert impedance[3] rather than Modified Warburg. (The Bisquert impedance corresponds to a transmission line model where the electrode has a finite resistance (like in Paasch's model[4]) and moreover has a CPE-type behavior in the electrode. In that model, we took $L/\lambda \rightarrow (L/\lambda)^{\phi}$, to fix the low-frequency CPE behavior). Good fits can also be obtained in that case, but that model has two more fit parameters, and three of these fit parameters had enormous standard deviations.

Figure S3: Impedance spectroscopy data for Cell B. (a) Complex plane impedance plot. (b) Zoom in to the high-frequency regime of a panel (a). (c) The real and imaginary part of the impedance versus frequency.
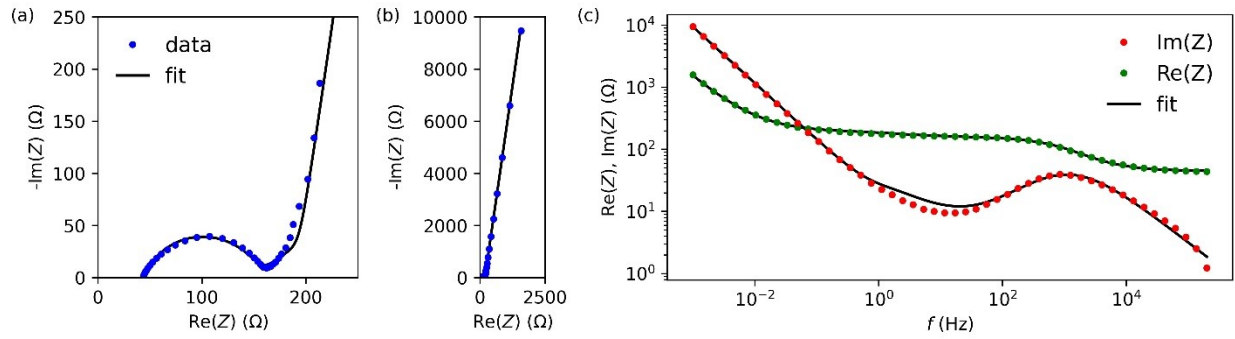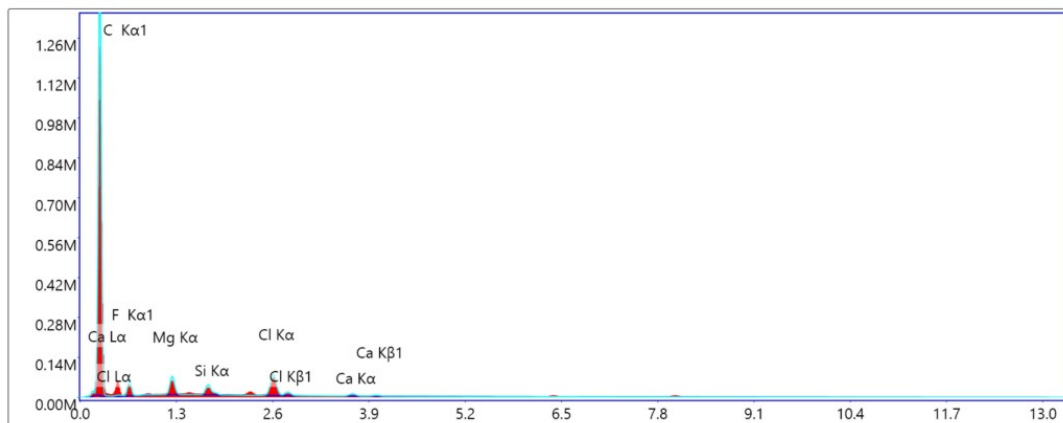
Figure S4: EDX spectra of ACCu1 sample after cycling studies.

Element	Weight %	Atomic %	Error %	Kratio	Z	A	F
C K	89.8	94.7	5.7	0.4752	1.0129	0.0522	1.0000
F K	4.5	3.0	9.3	0.0080	0.8988	0.2013	1.0000
Mg K	1.7	0.9	4.4	0.0106	0.8919	0.6828	1.0036
Si K	0.8	0.4	2.3	0.0064	0.8771	0.9035	1.0092
Cl K	2.7	1.0	1.5	0.0231	0.8165	1.0219	1.0159
Ca K	0.5	0.2	2.5	0.0041	0.8269	1.0308	1.0374

Formulae used in supercapacitor studies

Specific capacitance from CV technique:

The specific capacitance (Cs) was calculated using equation S1:

$$C_s = 2[ms(V_a - V_b)]^{-1} \int I(V)\, dV \qquad \text{(S1)}$$

where, s is the scan rate, $(V_a - V_b)$ refers to the working potential range, and m is the mass of the active material taken in a single electrode.

The active mass of all the samples was in the range of ~1.5 mg. The area of the electrode material was fixed to 1 cm^2.

Specific capacitance from the GCD technique:

The specific capacitance from the galvanostatic charge-discharge of the electrode is obtained using the equation S2:

$$C_s = \frac{4\,(I \times \Delta)}{(\Delta V \times m)} \qquad \text{(S2)}$$

Energy density and Power Density

The specific energy of the cells was calculated by using the expression:

$$E = \frac{1}{2} C_d V^2 \qquad \text{(S3)}$$

The specific power of the cells was calculated as:

$$P = E/\Delta t \qquad \text{(S4)}$$

Formulae used in dye adsorption studies

Amount of dye adsorption on a carbon surface

$$Q = \frac{(C_0 - C_x) \times V}{m}$$

(S5)

where: Q (mg·g⁻¹) is the amount adsorbed, C_0 (ppm) is the initial concentration of Malachite green, Cx (ppm) is concentration of MG after adsorption, V (L) is the volume of the solution, m (g) is the mass of the adsorbent.

The effectiveness of adsorption MG was calculate applying equation (S7):

$$\%H = \frac{(C_0 - C_x)}{C_0} \, x \, 100\%$$

(S6)

where: %H is the effectiveness of the adsorption process (%).

Equations used for kinetic studies

Equations (S8) and (S9) express pseudo-first and pseudo-second kinetic orders, respectively.

$$loglog \, (Q_e - Q_t) = \frac{-k_1}{2.303}t + loglog \, Q_e$$

(S7)

$$\frac{t}{Q_t} = \frac{1}{k_2 Q_e^2} + \frac{t}{Q_e}$$

(S8)

where: Q_e (mg g⁻¹) is the equilibrium of adsorption capacity, Q_t (mg g⁻¹) is the amount of adsorbent in time within adsorption process, t (min) is the adsorption lead time, k_1 (min) is the pseudo-first kinetic order constant, k_2 (g mg⁻¹ min⁻¹) is the pseudo-second kinetic order constant.

Isotherm equations

$$Q_e = \frac{Q_{max} C_e K_L}{(1 + C_e K_L)}$$

(S9)

$$Q_e = K_F C_e^{1/n} \qquad \text{(S10)}$$

$$Q_e = \frac{K_{RP} C_e}{(1 + a_{RP} C_e^{g})} \qquad \text{(S11)}$$

where: Q_{max} (mg g^{-1}) is the maximal adsorption capacity, C_e (mg L^{-1}) is the equilibrium concentration of dye in the solution, K_L (L mg^{-1}) is the Langmuir constant, K_F (mg g^{-1})(dm^3 g^{-1})^n is the adsorption capacity Freundlich constant, n is the heterogeneity factor or favourability of adsorption, K_{RP}, a_{RP} (L g^{-1}), (mg L^{-1})$^{-g}$ is the Redlich-Peterson constant and g is the dimensionless factor.

Table S1: Comparison of adsorption capacity of MG with different materials.

Material	Q_{max} (mg g^{-1})	References
Acid-activated carbon from coconut shell	32.787	5
SA@GG@B composites	47.16	6
Pithophora sp.	117.647	7
MOF-5/RHA&CFA/2:1	39.47	8
MFA	112.20	9
NSC	23.75	10
ACCu1	**153.16**	**This work**

References

1 J. Song and M. Z. Bazant, Effects of Nanoparticle Geometry and Size Distribution on Diffusion Impedance of Battery Electrodes, *J Electrochem Soc*, 2013, **160**, A15–A24.

2 A. Lasia, in *Electrochemical Impedance Spectroscopy and its Applications*, Springer New York, New York, NY, 2014, pp. 85–125.

3 J. Bisquert, G. Garcia-Belmonte, F. Fabregat-Santiago and A. Compte, Anomalous transport effects in the impedance of porous film electrodes, *Electrochem Commun*, 1999, **1**, 429–435.

4 G. Paasch, K. Micka and P. Gersdorf, Theory of the electrochemical impedance of macrohomogeneous porous electrodes, *Electrochim Acta*, 1993, **38**, 2653–2662.

5 R. S. piriya, R. M. Jayabalakrishnan, M. Maheswari, K. Boomiraj and S. Oumabady, Comparative adsorption study of malachite green dye on acid-activated carbon, *Int J Environ Anal Chem*, 2023, **103**, 16–30.

6 N. Iqbal, S. A. Al-Hussain, F. Batool, A. Mumtaz, A. Irfan, S. Noreen, M. Mustaqeem and M. E. A. Zaki, Alginate-Based Sustainable Green Composites of Polymer and Reusable Birm for Mitigation of Malachite Green Dye: Characterization and Application for Water Decontamination, *Sustainability*, 2023, **15**, 3194.

7 K. V. Kumar, S. Sivanesan and V. Ramamurthi, Adsorption of malachite green onto Pithophora sp., a fresh water algae: Equilibrium and kinetic modelling, *Process Biochem.*, 2005, **40**, 2865–2872.

8 I. Dahlan, O. H. Keat, H. A. Aziz and Y.-T. Hung, Synthesis and characterization of MOF-5 incorporated waste-derived siliceous materials for the removal of malachite green dye from aqueous solution, *Sustain Chem Pharm*, 2023, **31**, 100954.

9	K. Singh, A. Kumar, A. K. Singh and A. Agarwal, Fly ash and TiO_2 modified fly ash as adsorbing materials for effective removal of methylene blue and malachite green from aqueous solutions, *J. Indian Chem. Soc.*, 2023, **100**, 100942.

10	A. Naboulsi, A. Kassimi, H. Yazid, F. Essebbar, M. El Himri and M. El Haddad, Adsorption of single and mixed colors by kaolinite clay: Experimental research combined with a theoretical examination using DFT, *J Mol Struct*, 2023, **1276**, 134687.